Contents list available at CBIORE journal website

International Journal of Renewable Energy Development

Journal homepage: https://ijred.cbiore.id

Research Article

Drying turmeric slices using a photovoltaic ventilation direct solar dryer: Drying characteristics and interactions of heat and mass transfer

Bambang Waluyo Hadi Eko Prasetiyono[a], Suherman Suherman[b*], Bakti Jos[b], Muhammad Anas Asy-Syaqiq[b]

[a]*Department of Animal Science, Faculty of Animal and Agricultural Science, Diponegoro University, Tembalang, Semarang, Central Java, 50275, Indonesia*

[b]*Department of Chemical Engineering, Faculty of Engineering, Diponegoro University, Tembalang, Semarang, Central Java, 50275, Indonesia*

Abstract. This study compares the drying characteristics and the heat and mass transfer phenomena while drying turmeric slices using a photovoltaic ventilation direct solar dryer and open sun drying. Turmeric slices of varying thicknesses—5, 7, and 10 mm—were dried from 83.48% to a final moisture content of 5–6% to ensure safe storage conditions. The drying times required were 1440, 1800, and 2160 min for the direct solar dryer, and 2220, 2520, and 2880 min for open sun drying at 5, 7, and 10 mm thicknesses, respectively. Drying Turmeric slices using the direct solar dryer at thinner thicknesses showed a faster drying rate, with the highest average drying rate observed for the 5 mm slices at 0.287 g/min. Similarly, drying efficiency was higher for thinner slices. The Midilli model provided the best fit for experimental and predicted data in describing the drying kinetics of turmeric slices. The effective moisture diffusivity obtained in this study was 1.65×10^{-8}, 2.66×10^{-8}, and 4.11×10^{-8} m^2/s for the direct solar dryer, and 0.89×10^{-8}, 1.52×10^{-8}, and 2.38×10^{-8} m^2/s for open sun drying at 5, 7, and 10 mm thicknesses, respectively. Higher heat and mass transfer coefficients were observed for drying thinner turmeric slices using the direct solar dryer. The convective heat transfer and evaporative heat transfer coefficients decreased as the moisture content was reduced. In contrast, the mass transfer coefficient increased as the drying time progressed.

Keywords: Drying Characteristics, Energy Analysis, Heat and Mass Transfer, Solar Drying, Turmeric Slices

Received: 20th January 2025; Revised: 18th Feb 2026; Accepted: 11th July 2026; Available online: 27th July 2026

1. Introduction

Turmeric (*Curcuma longa*) is a spice plant commonly found in tropical and subtropical regions of Asia and the Middle East (Sharma *et al.,* 2021). In 2023, turmeric production in Indonesia reached 205.65 million kilograms, contributing 3% of the world's total production (BPS, 2024; Turmeric outlook, 2024). Turmeric is used in cooking for its flavor and potential health benefits, as it contains the active compound curcumin. The rhizomes of turmeric are rich in antioxidants and bioactive compounds that support wound healing, burns, and various conditions such as fever, cough, colds, gastrointestinal issues, colic, arthritis pain, inflammation, stomach ulcers, and offer protective effects for the liver and kidneys. Curcumin, the main active component in turmeric, consists of diferuloylmethane, desmethoxycurcumin, and bisdemethoxycurcumin. It plays multiple roles in health as a food additive, coloring agent with its characteristic orange-yellow color, therapeutic agent, and medicine. Curcumin is renowned for its medicinal properties, including anti-inflammatory, antimicrobial, anticancer, and anti-HIV activities (Dutta *et al.,* 2023). During sun-drying, it has been reported that a significant amount of curcumin can degrade, up to nearly 72% (Komonsing *et al.*, 2022). Therefore, processing turmeric poses substantial challenges in preserving its phytonutrients and quality value.

The drying process requires a significant amount of energy, primarily relying on fossil fuel-based electricity, which is expensive and unsustainable for farmers (Madhankumar *et al.*, 2023). In developed countries, drying consumes 12 – 40% of industrial energy and 20 – 70% of production costs. Solar energy can reduce the use of non-renewable resources by 27 – 80% (Lingayat *et al.,* 2021). Additionally, Indonesia is located along the equator and benefits from high solar radiation of 5 $kW/h.m^2$ throughout the year (Hasan Masud et al., 2020). Solar drying has long been introduced as a food preservation method and is widely applied in various countries. A simple solar dryer typically consists of a box-shaped chamber with a transparent glass cover for drying food (Jha & Tripathy, 2021). The primary targets for simple solar drying technology are personal use, rural agriculture, and small-scale industries in developing regions such as Indonesia, Malaysia, India, and parts of Africa and Southeast Asia. Enhancing this technology is essential for industrial use, as solar energy provides a clean and renewable resource for thermal processes (Lingayat *et al.,* 2022).

Advancements in research related to the development and optimization of solar drying technology to enhance the utilization of solar energy have been studied by researchers. Various modifications and improvements have been applied to solar drying technology for various food products. Examples

* Corresponding author
Email: suherman.mz@che.undip.ac.id (S. Suherman)

include drying ginger and cassava starch using hybrid solar dryers integrated with LPG burners (Suherman *et a*l., 2020, 2021), drying turmeric using mixed solar dryers with double solar air collectors and thermal energy storage systems (Lakshmi *et al.,* 2018), drying tomatoes using hybrid solar dryers with compound parabolic concentrator flat plate collectors and auxiliary heaters (Ebadi *et al*., 2021), drying potatoes using indirect solar dryers assisted by single flat plate solar collectors and phase change materials (Vigneshkumar *et al*., 2021), drying red chilies using indirect solar dryers with natural heat storage systems (Arunkumar *et al*., 2024), and drying tomatoes, ginger, and bottle gourd using greenhouse solar dryers integrated with evacuated tube solar collectors (Singh & Gaur, 2021), among others. Some of the modifications applied in previous studies require high initial investment costs and may not be sustainable for local farmers. Therefore, this study developed, constructed, and evaluated the performance of a simple direct solar dryer powered by photovoltaic (PV) panels, making it suitable for small-scale farmers. Turmeric, a significant spice in Indonesia, was chosen to evaluate the system's performance under various material thickness conditions. Drying characteristics parameters, such as moisture content, drying rate, and drying efficiency, were used to determine the impact of drying operational conditions on turmeric slices. Additionally, mathematical modeling was conducted to describe the drying behavior of turmeric slices using a photovoltaic ventilation direct solar dryer.

Mathematical modeling is an essential tool with the potential to describe and predict the drying characteristics of food products, identify factors influencing drying efficiency performance, and minimize operational costs (Perussello *et al.,* 2012). Thin-layer modeling provides insights into drying kinetics over time under specific drying conditions, which affect drying efficiency and the final product quality (Gasa et al., 2022). Various thin-layer model equations from the literature are selected and experimentally fitted to the drying curves in solar drying. These models are then validated using statistical analysis to determine the best fit and the model's ability to predict the mass loss of food products under the proposed drying variable conditions. Therefore, thin-layer drying modeling analysis is necessary to understand the effects of drying conditions on drying behavior and performance. In this study, the focus is on variations in the thickness of turmeric slices.

Heat transfer during drying occurs through convection, while mass transfer happens through diffusion, driven by temperature and moisture concentration gradients. Studies on heat and mass transfer are crucial, particularly in dryer design, to determine drying performance parameters such as efficiency, cost, and product quality (Koua *et al.,* 2019). Drying is a complex process that involves the simultaneous interaction of mass and heat transfer. The diverse morphological properties of food products as drying materials significantly impact their drying behavior, making mathematical modeling a challenging task (Perussello *et al.,* 2014). Most models applied are based on Fick's law to represent the transient phenomenon of mass transfer and the analysis of dimensionless numbers (Nusselt number, Prandtl number, Grashof number for natural convection, and Reynolds number for forced convection) to understand heat transfer phenomena (Jain, 2006; Kern, 1965). Therefore, this study was conducted to determine the heat and mass transfer coefficients for various thicknesses of turmeric slices under natural convection conditions in a direct solar dryer.

2. Materials and methods

2.1 Solar dryer description

A photovoltaic direct solar dryer with ventilation was designed and developed, as shown in Figures 1 and 2. The drying chamber is box-shaped, made of stainless steel, with a transparent glass cover measuring 50 cm (length) x 40 cm (width), equipped with an exhaust fan and three 4 cm diameter ventilation holes on each side (right and left). The drying chamber is placed on a metal stand with wheels to facilitate mobility. Inside the drying chamber, there is a tray measuring 30 x 30 cm made of wire mesh and stainless steel on the edges to hold the drying material. The transparent glass cover is mounted with hinges, allowing it to be opened and closed like a window. The intake air flows naturally from the surrounding environment through the ventilation holes. The exhaust air is driven by a 4-inch fan (19.5 x 14.5 x 19.5 cm) powered by electricity from a PV panel.

Data collection during the drying process is conducted every hour. The measuring instruments used to read the surrounding weather conditions include the solar power meter SM-206 to measure solar intensity (Accuracy: ±10 W/m^2 or ±5% of the measured value), the Smart Sensor AS847 humidity & temperature meter to measure temperature and relative humidity (Accuracy: ±3.5 %RH and ±3 °C), and the Krisbow

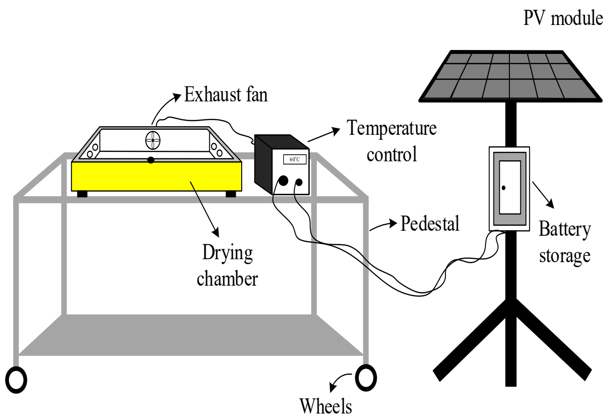

Fig. 1 Schematic of photovoltaic ventilation direct solar dryer

Fig. 2 3D views of ventilation direct solar dryer

Electronic Kitchen Digital Scale 5 kg Slim Plate to weigh the samples before and after drying (Accuracy: ±0.1 g).

2.2 Drying procedure

Fresh turmeric, recently harvested, was purchased from local farmers in Semarang Regency and cleaned with running water to remove surface dust. It was then immersed in hot water at 80-85 °C for about 2 minutes. Subsequently, the product was removed from the hot water and allowed to air dry at room temperature to eliminate surface moisture. The turmeric was sliced into cylindrical shapes using a kitchen knife with a diameter of 30-35 mm, with varying thicknesses of 5, 7, and 10 mm. A sample weighing 500 g was selected and placed on a drying tray. The weight of the sample was measured at 60-minute intervals using an electronic scale. The experiment was conducted in one day, starting from 09:00 AM to 04:00 PM, and continued the following day to study the drying behavior of the product. At the beginning of the drying experiment, the solar dryer was calibrated for 15-20 minutes without a load to achieve stable conditions. The turmeric slices were evenly spread on a wire mesh rack to ensure that the diffusion process occurred homogeneously. Ambient air flowed through the tray while being heated by solar radiation to remove moisture from the turmeric slices. The weight of the turmeric slices was measured every hour during the drying process. Similarly, data collection on the surrounding weather conditions and the solar dryer was also conducted using the available measuring instruments. The drying of the turmeric slices was stopped when the final moisture content reached 5-6% wb to ensure safe storage (Borah et al., 2015). The initial moisture content of the turmeric slices was measured using the oven method at a temperature of 105 °C for 24 hours and was determined using equation (1) (Hssaini *et al.,* 2021).

$$MC_i = \frac{W_i - W_f}{W_i} \times 100\% \ (wet\ basis) \tag{1}$$

where: MC_i is the initial moisture content of the turmeric slices (% wb), W_i is the initial weight of the turmeric slices (g), W_f is the final weight of the turmeric slices (g).

2.3 Data processing analysis

2.3.1 Drying characteristics

The moisture content of the turmeric slices during drying using a direct solar dryer can be calculated using equation (2) (Suherman *et al.,* 2024).

$$MC_t = \frac{W_w - W_d}{W_w} \tag{2}$$

where: MC_t is the moisture content of the turmeric slices at time t on wet basis (% wb), W_w is the wet weight of the turmeric slices during the drying time interval (g), W_f is the dry weight of the turmeric slices (g).

The drying rate is estimated using equation (3) because it provides high accuracy (Efendi, 2024).

$$DR = \frac{W_{(t+\Delta t)} - W_t}{\Delta t} \tag{3}$$

where: DR is the drying rate (g/min), $W_{t+\Delta t}$ is the weight of the material at time t+ Δt (g), W_t is the weight of the material at time t (g).

The drying efficiency (η_d) can be expressed as the ratio of the thermal energy required to remove moisture from the sample to the total thermal energy input into the dryer over the time interval, as stated in equation (4) (Deepak & Behura, 2025).

$$\eta_d = \frac{m_{evp}\lambda}{I A_d \Delta t} \tag{4}$$

where: η_d is the drying efficiency (%), m_{evp} is the total mass of the evaporated product (kg), λ is the latent heat of the drying air (kJ/kg), I is the solar intensity (W/m^2), A_d is the surface area of the glass collector in the drying chamber (m^2), and Δt is the drying time difference (s).

2.3.2 Thin-layer modeling

The drying kinetics evaluation of turmeric slices involves changing the value of the dimensionless moisture ratio (MR), which can be expressed in equation (5) (Poonia et al., 2018).

$$MR = \frac{MC_t - MC_e}{MC_i - MC_e} \tag{5}$$

Let, the equilibrium moisture content (MC_e) has a small value, allowing it to be neglected and simplified into equation (6).

$$MR = \frac{MC_t}{MC_i} \tag{6}$$

Thin layer modeling is widely and effectively applied to describe the drying mechanism models of food. Among the various thin-layer drying models available, eight models were selected for consideration and comparison in this study, as presented in Table 1. Furthermore, these models were examined to provide the most suitable empirical relationships, demonstrating a good fit by evaluating the highest estimated values of the coefficient of determination (R^2) and the lowest root mean square error (RMSE), as expressed in Appendix A (Chicco *et al.,* 2021; Gasa *et al.,* 2022).

Table 1
Application of the thin layer drying model for the drying kinetics of turmeric slices

No	Model name	Model equation
1	Newton	$MR = \exp(-kt)$
2	Handerson-Pabis	$MR = a\exp(-kt)$
3	Page	$MR = \exp(-kt^n)$
4	Modified page	$MR = \exp(-kt)^n$
5	Midilli	$MR = a\exp(-kt^n) + bt$
6	Modified Midilli	$MR = a\exp(-kt^n) + b$
7	Logarithmic	$MR = a\exp(-kt) + c$
8	Aghbashlo	$MR = \exp\left(-\frac{k_1 t}{1+k_2 t}\right)$

2.3.3 Effective moisture diffusivity

The phenomenon of effective moisture diffusion describes a crucial parameter in the transport model of moisture flow within food-drying products. The movement of moisture from within the product to the outer surface is influenced by various interacting transport mechanisms, such as capillary flow, Knudsen diffusion, surface diffusion, evaporation and condensation, and pure diffusion. This moisture is then evaporated by hot air through convection. Fick's second law is generally used to express the phenomenon of moisture diffusion and to analyze the drying behavior during the falling rate period, as stated in equation (9) (Koukouch *et al.,* 2017).

$$\frac{\partial MR}{\partial t} = D_{eff}\nabla^2 MR \quad (9)$$

The diffusivity analysis assumes that moisture transport occurs through a diffusion process with a uniform concentration, where internal moisture movement becomes the resistance, there are no barriers to heat and mass transfer from the outside, and the effective diffusion coefficient remains constant. The equation is derived from the theoretical model of Fick's law, which can be formulated in equation (10) to identify the diffusivity in plate geometry samples (Khater *et al.,* 2024).

$$MR = \frac{8}{\pi^2}\sum_{n=1}^{\infty}\frac{1}{n^2}\exp\left(\frac{-\pi^2 D_{eff} t}{4L^2}\right) \quad (10)$$

Equation (10) is simplified into the form of equation (11), and subsequently, the equation is linearized by multiplying both sides by the natural logarithm, resulting in equation (12) (Tagnamas et al., 2024).

$$MR = \frac{8}{\pi^2}\exp\left(\frac{-\pi^2 D_{eff}}{4L^2}t\right) \quad (11)$$

$$\ln(MR) = \ln\left(\frac{8}{\pi^2}\right) - \left(\frac{-\pi^2 D_{eff}}{4L^2}\right)t \quad (12)$$

where: D_{eff} is the effective moisture diffusivity (m^2/s), t is drying time (s), n is a positive integer, L is the half-thickness of samples (m).

The effective moisture diffusivity (D_{eff}) can be calculated using a linear equation, where plotting the data of ln(MR) against time (t) will yield a straight-line curve. From the straight-line equation, the slope can be determined to calculate the value of D_{eff} using equation (13).

$$slope = \frac{-\pi^2 D_{eff}}{4L^2} \quad (13)$$

2.3.4 Convective heat and mass transfer

The convective heat transfer coefficient (h_c) is investigated for drying turmeric slices using natural convection flow. The heat transfer calculations are determined by assuming the product temperature remains constant (T_{ps}) and that the length of the product (L) is too short to allow for turbulent flow (Daş et al., 2021). The Nusselt number (Nu) for natural convection is expressed as a function of the Grashof number (Gr) and the Prandtl number (Pr). A single equation can correlate a consistent relationship for laminar and turbulent regimes, as shown in equation (14) (Jain, 2006; Malik & Kumar, 2024b; Shimpy *et al.*, 2024).

$$Nu = \frac{h_c L}{K_v} = C(GrPr)^n \quad (14)$$

Then, the value of h_c can be determined using equation (15).

$$h_c = \frac{K_v}{L}C(GrPr)^n \quad (15)$$

The heat required to evaporate the moisture is expressed in equation (16).

$$Q_e = 0.016h_c\left[P(T_{ps}) - \gamma P(T_{aps})\right] \quad (16)$$

Equation (16) is substituted into equation (15), resulting in the equation written as equation (17).

$$Q_e = 0.016\frac{K_v}{L}C(GrPr)^n\left[P(T_{ps}) - \gamma P(T_{aps})\right] \quad (17)$$

The total mass of moisture evaporated (m_{evp}) from the turmeric slices in the direct solar dryer through natural convection can be calculated by equation (18).

$$m_{evp} = 0.016\frac{K_v}{\lambda L}C(GrPr)^n\left[P(T_{ps}) - \gamma P(T_{aps})\right]A_p t \quad (18)$$

Equation (19) can be simplified by assuming $Z = 0.016\frac{K_v}{\lambda L}\left[P(T_{ps}) - \gamma P(T_{aps})\right]A_p t$ and can be expressed in equation (19).

$$\frac{m_{evp}}{Z} = C(GrPr)^n \quad (19)$$

Equation (19) is linearized by multiplying the natural logarithm of both sides, resulting in equation (20). By the linear regression method, $y = mx + c$, the values of the constants (C and n) can be calculated using equation (20), and subsequently, the value of h_c can be determined using equation (15).

$$\ln\left(\frac{m_{evp}}{Z}\right) = n\ln(GrPr) + \ln C \quad (20)$$

The evaporative heat transfer coefficient (h_e) can be calculated using equation (21).

$$h_e = 0.016h_c\left[\frac{P(T_{ps}) - \gamma P(T_{aps})}{T_{ps} - T_{aps}}\right] \quad (21)$$

Appendix B shows how the Grashof number (Gr), Prandtl number (Pr), and the thermophysical properties of air were determined.

The convective mass transfer coefficient (h_m) is an effective parameter in expressing the drying behavior, providing a good understanding of the physics of drying (Daş *et al.,* 2021; Koua *et al.,* 2019). The value of h_m can be calculated using equation (22).

$$h_m = \frac{V}{A_p t}\ln(MR) \quad (22)$$

where: h_m is the mass transfer coefficient (m/s), V is the volume of the material (m^3), A_p is the surface area of the material (m^2), and the shape of turmeric slices is the assumption of cylindrical.

2.3.4 Statistical analysis

Each variable variation was conducted in triplicate, and data such as ambient temperature and relative humidity (input), material surface temperature (dryer), temperature above the material surface (output), solar radiation intensity, and sample weight were recorded as mean values and standard deviations. One-way ANOVA was applied to analyse the data, with statistical significance determined at a threshold of $p < 0.05$ using Microsoft Excel software. The detailed parameters of the ANOVA calculation are presented in Appendix C.

3. Results and discussion

3.1 Moisture content curve analysis

The initial moisture content of the turmeric slices was 83.48%, which was reduced using two different drying methods to reach the final moisture content at 5, 7, and 10 mm thickness of 5.35%, 5.27%, and 5.48% for the direct solar dryer with photovoltaic ventilation, and 7.85%, 8.43%, and 9.85% for open sun drying, respectively, as shown in Figure 3. The drying time required to reach the final moisture content of 5, 7, and 10 mm in the photovoltaic ventilation direct solar dryer and open sun drying were 1440 min, 1800 min, 2160 min, 2220 min, 2520 min, and 2880 min, respectively. The direct solar dryer was able to shorten the drying time to 720 – 780 minutes compared to the open solar drying method due to the higher temperature reached in the drying chamber, thus increasing the potential and importance of the direct solar dryer. The ANOVA results of the effect of slices on the reduction of moisture content using both the photovoltaic ventilation direct solar dryer and open sun drying showed significant differences ($P < 0.05$), as displayed in Table 2. This indicates that the thickness of turmeric slices significantly affects the drying process. Dried turmeric slices have a porous surface that allows for better exposure to drying air (Borah *et al.,* 2015). In addition, thinner slices have a larger surface area, accelerating heat transfer and increasing water evaporation (Jeevarathinam *et al.,* 2021). In contrast, thicker materials prolong the drying duration as the distance required for the water diffusion process from the inside of the material to the outside surface becomes longer (Hasibuan *et al*., 2025). Therefore, drying turmeric slices at thinner thicknesses has been shown to reduce drying duration, and energy consumption for drying can be further saved.

3.2 Drying rate curve analysis

Figure 4 illustrates the drying rate phenomenon of turmeric slices using a photovoltaic ventilation direct solar dryer and open sun drying method. During the initial drying period, there is an adjustment or initial heating phase, where the sample has a lower temperature than the final temperature, resulting in an increased drying rate during the first 2 to 3 hours (Bhaskara Rao & Murugan, 2021). The high moisture content of the sample at the beginning of the drying period enhances the sample's ability to absorb solar radiation heat, creating a pressure difference between the interior and the surface of the sample, which accelerates the movement of moisture diffusion and the friction forces between molecules within the sample. Subsequently, the drying rate curve primarily exhibits a declining trend over time as the moisture content in the sample evaporates during the drying process (Jeevarathinam *et al.,* 2021). The effect of slice thickness and drying method on the average drying rate showed a significant difference ($P < 0.05$) based on the ANOVA results,

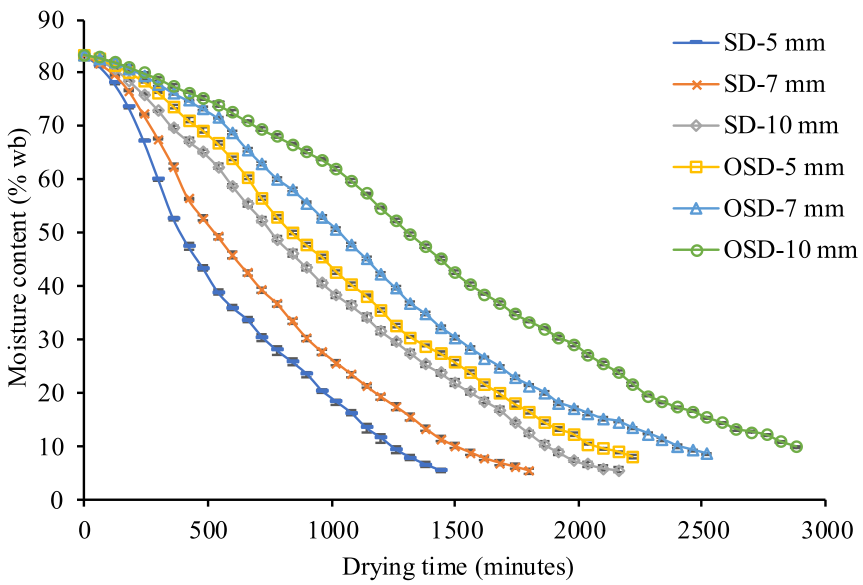

Fig. 3 Moisture content curve of turmeric slices

Table 2
ANOVA results for the moisture content reduction

Source of variation	SS	df	MS	F	P-value	F-crit
Between groups	18746.91	5	3749.38	10.03	2.45×10^{-8}	2.27
Within groups	58328.72	156	373.90			
Total	77075.63	161				

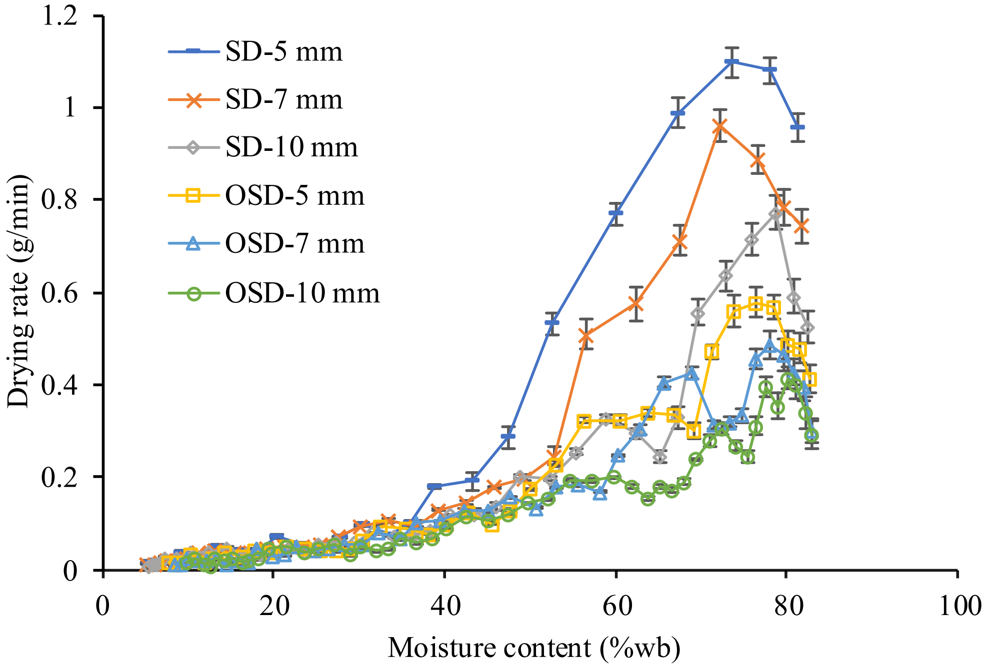

Fig. 4 Drying rate curve of turmeric slices

Table 3
ANOVA results for the average drying rate

Source of variation	SS	df	MS	F	P-value	F-crit
Between groups	0.04	5	0.008	276658.5	6.25 x 10^{-30}	3.11
Within groups	3.50 x 10^{-7}	12	2.92 x 10^{-8}			
Total	0.04	17				

as presented in Table 3. The photovoltaic ventilation direct solar dryer has the highest average drying rates with thinner slices of 0.287, 0.229, and 0.191 g/min. In contrast, the open sun drying method had lower drying rates of 0.185, 0.163, and 0.142 g/min for thicknesses of 5, 7, and 10 mm, respectively. As previously explained, thinner slices have a larger surface area, allowing for faster heat and mass transfer within the sample (Sun et al., 2025). These results are generally consistent with previous studies regarding the effect of sample thickness on drying rates, including the drying of olive pomace at thicknesses of 2, 4, and 6 cm (Abderrahman *et al.*, 2022), Gardenia erubescent fruit at thicknesses of 3 and 5 mm (Korese & Achaglinkame, 2024), and yam slices at thicknesses of 3, 5, and 7 mm (Shen *et al.,* 2024).

3.3 Drying efficiency curve analysis

The drying efficiency curve of turmeric slices at various thicknesses using different drying methods is shown in Figure 5. The drying efficiency during the initial period is higher than the subsequent time until the end. This trend indicates decreasing drying efficiency as the drying operation time increases due to the reduction in moisture content of the turmeric slices until the end of the drying period, which leads to a decline in efficiency (Admass *et al.,* 2024; Kerse *et al.,* 2025). The average drying efficiency obtained during the drying process using the direct solar dryer was 5.22%, 4.27%, and 3.91%, respectively, while the drying efficiency using the open sun drying method was 3.70%, 3.07%, and 2.64% for 5, 7, and 10 mm thickness, respectively. The average drying efficiency results at various slice thicknesses using different drying methods showed a significant difference ($P < 0.05$) based on the ANOVA test, as shown in Table 4. The drying efficiency for 5 mm thickness is higher compared to thicker slices. Thinner slices can remove more water during the initial drying period, significantly increasing drying efficiency. Furthermore, the direct solar dryer yielded higher drying efficiency results than open solar drying, as the higher temperature in the drying chamber resulted in greater moisture removal and thus increased drying efficiency. However, the efficiency results found in this study are still relatively low due to the small drying chamber that limits the loading capacity of the dried turmeric slices and the solar radiation energy that goes partially unused, leading to wasted energy and reduced drying efficiency (Choudhary & Hazarika, 2024; Suherman *et al.*, 2024).

3.4 Thin-layer drying modeling

Regression analysis for various thin layer drying models was conducted by correlating experimental data to predict the dimensionless moisture ratio (MR) as a function of drying time at different turmeric slice thicknesses (5, 7, and 10 mm). The equations presented in Table 1 were calculated using the DrYFiT software (Drying Data Fitting Tool): a Microsoft Excel Freeware Tool created by (Öksüz & Buzrul, 2024). Statistical parameters, such as the coefficient of determination (R^2) and Root Mean Square Error (RMSE), were applied to validate the

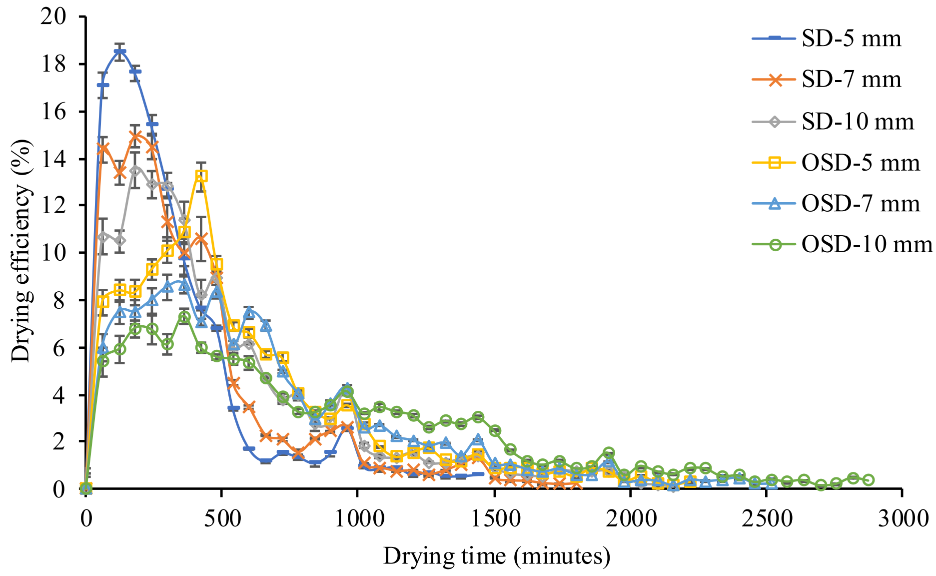

Fig. 5 Drying efficiency curve of turmeric slices using photovoltaic ventilation direct solar dryer and open sun drying at various thickness variations

Table 4
ANOVA results for the average drying efficiency

Source of variation	SS	df	MS	F	P-value	F-crit
Between groups	12.41	5	2.48	6929.53	2.52×10^{-20}	3.11
Within groups	4.30×10^{-3}	12	3.58×10^{-4}			
Total	12.42	17				

best-fitting model. The results of the model constant calculations and statistical analysis are presented in Table 5. Most of the selected thin-layer drying models showed a good fit with the experimental data distribution, as indicated by R^2 values greater than 0.9950, except for the Lewis (Newton), Henderson and Pabis, Logarithmic (for all variables except the direct solar dryer at 7 mm and 10 mm thickness) and the Aghbashlo models (for all variables except the direct solar dryer at 7 mm and 10 mm thickness). However, the Midilli model provided the most accurate representation of the drying process for all drying methods and turmeric slice thickness variations based on statistical analysis. This model showed the highest statistical parameter values of R^2 (0.9963, 0.9991, and 0.9994 for direct solar dryer, and 0.9994, 0.9998, and 0.9990 for open sun drying at thicknesses of 5, 7, and 10 mm, respectively) and the lowest RMSE values (0.0198, 0.0100, and 0.0077 for direct solar dryer, and 0.0076, 0.0049, and 0.0095 for open sun drying at thicknesses of 5, 7, and 10 mm, respectively). The constant values obtained in the Midilli model are expressed in equations (23) to (28).

For solar dryer – 5 mm:
$$MR = 1.0281 \exp(-0.0004t^{1.1964}) + (-1.99 \times 10^{-5}t) \quad (23)$$

For solar dryer – 7 mm:
$$MR = 1.0172 \exp(-0.0001t^{1.3074}) + (-1.35 \times 10^{-5}t) \quad (24)$$

For solar dryer – 10 mm:
$$MR = 1.0061 \exp(-5.08 \times 10^{-5}t^{1.3705}) + (-4.44 \times 10^{-5}t) \quad (25)$$

For open sun drying – 5 mm:
$$MR = 1.0044 \exp(-1.25 \times 10^{-5}t^{1.5664}) + (-8.15 \times 10^{-6}t) \quad (26)$$

For open sun drying – 7 mm:
$$MR = 0.9909 \exp(-2.25 \times 10^{-6}t^{1.7863}) + (-1.54 \times 10^{-5}t) \quad (27)$$

For open sun drying – 10 mm:
$$MR = 0.9811 \exp(-6.43 \times 10^{-7}t^{1.8883}) + (-2.32 \times 10^{-6}t) \quad (28)$$

The Midilli model includes both an exponential decay component and a linear term. This combination provides the flexibility to model both the early rapid drying phase and the slower final stage, which are commonly seen in thin-layer drying processes. With four parameters (a, b, k, and n), the Midilli model offers greater adaptability compared to simpler models like Lewis or Henderson and Pabis. This allows for better fitting to experimental data across a range of drying conditions and sample thicknesses (Ambawat *et al.*, 2022; Midilli *et al.*, 2002). The selected Midilli model is validated by comparing the experimental moisture ratio values with the predicted moisture ratios in Figure 6. The curve shows that the predicted MR values closely match the experimental data, indicated by a straight line forming a 45° angle, supported by high R^2 values of 0.9988, 0.9997, and 0.9998 for direct solar dryer, and 0.9994, 0.9998, and 0.9990 for open sun drying at thicknesses 5, 7, and 10 mm, respectively. Therefore, the Midilli model indicates the best fit for describing the drying behavior of turmeric slices.

3.5 Effective moisture diffusivity

Effective moisture diffusivity is a material parameter that describes the mechanism of moisture transfer from wet products. The value of moisture diffusivity is influenced by

Table 5
Results of the calculated model constant values obtained and statistical parameter analysis

Model Name	Drying method	Thickness (mm)	Model constant	R^2	RMSE
Lewis (Newton)	SD	5	k = 0.0014	0.9736	0.0491
		7	k = 0.0011	0.9656	0.0570
		10	k = 0.0008	0.9453	0.0712
	OSD	5	k = 0.0007	0.9310	0.0783
		7	k = 0.0006	0.9195	0.0861
		10	k = 0.0005	0.9026	0.0924
Handerson and Pabis	SD	5	k = 0.0016; a = 1.0961	0.9869	0.0353
		7	k = 0.0013; a = 1.1144	0.9833	0.0404
		10	k = 0.0009; a = 1.1266	0.9689	0.0545
	OSD	5	k = 0.0009; a = 1.1498	0.9646	0.0568
		7	k = 0.0008; a = 1.1636	0.9580	0.0628
		10	k = 0.0006; a = 1.1522	0.9423	0.0719
Page	SD	5	k = 0.0002; n = 1.2950	0.9959	0.0205
		7	k = 8.21E-05; n = 1.3859	0.9988	0.0109
		10	k = 2.06E-05; n = 1.5221	0.9980	0.0137
	OSD	5	k = 9.75E-06; n = 1.6057	0.9994	0.0077
		7	k = 4.31E-06; n = 1.6877	0.9995	0.0071
		10	k = 5.11E-07; n = 1.9222	0.9972	0.0154
Modified page	SD	5	k = 0.0014; n = 1.2950	0.9956	0.0205
		7	k = 0.0011; n = 1.3859	0.9988	0.0109
		10	k = 0.0008; n = 1.5221	0.9980	0.0137
	OSD	5	k = 0.0008; n = 1.6057	0.9994	0.0077
		7	k = 0.0007; n = 1.6877	0.9995	0.0071
		10	k = 0.0005; n = 1.8052	0.9986	0.0114
Midilli	SD	5	k = 0.0004; a = 1.0281; b = -1.99E-05; n = 1.1964	0.9963	0.0198
		7	k = 0.0001; a = 1.0172; b = -1.35E-05; n = 1.3074	0.9991	0.0100
		10	k = 5.08E-05; a = 1.0061; b = -4.44E-05; n = 1.3705	0.9994	0.0077
	OSD	5	k = 1.25E-05; a = 1.0044; b = -8.15E-06; n = 1.5664	0.9994	0.0076
		7	k = 2.25E-06; a = 0.9909; b = 1.54E-05; n = 1.7863	0.9998	0.0049
		10	k = 6.43E-07; a = 0.9811; b = 2.32E-06; n = 1.8883	0.9990	0.0095
Modified midilli	SD	5	k = 0.0004; a = 1.0631; b = -0.0356; n = 1.1966	0.9962	0.0199
		7	k = 0.0001; a = 1.0491; b = -0.0320; n = 1.3014	0.9990	0.0100
		10	k = 5.78E-05 a = 1.1574; b = -0.1517; n = 1.3410	0.9994	0.0078
	OSD	5	k = 1.33E-05; a = 1.0301; b = -0.0258; n = 1.5567	0.9994	0.0076
		7	k = 5.72E-06; a = 1.0237; b = -0.0206; n = 1.6440	0.9992	0.0087
		10	k = 9.11E-07; a = 1.0075; b = -0.0211; n = 1.8358	0.9990	0.0099
Logarithmic	SD	5	k = 0.0011; a = 1.2532; c = -0.1964	0.9947	0.0230
		7	k = 0.0008; a = 1.3413; c = -0.2783	0.9962	0.0195
		10	k = 0.0004; a = 1.8756; c = -0.8259	0.9972	0.0166
	OSD	5	k = 0.0003; a = 2.1155; c = -1.0466	0.9940	0.0236
		7	k = 0.0002; a = 2.2082; c = -1.1286	0.9899	0.0311
		10	k = 2.81E-05; a = 12.7463; c = -11.6898	0.9908	0.0289
Aghbashlo	SD	5	k1 = 0.0011; k2 = -0.0003	0.9924	0.0269
		7	k1 = 0.0008; k2 = -0.0003	0.9952	0.0216
		10	k1 = 0.0005; k2 = -0.0003	0.9972	0.0164
	OSD	5	k1 = 0.0004; k2 = -0.0003	0.9929	0.0255
		7	k1 = 0.0004; k2 = -0.0003	0.9891	0.0319
		10	k1 = 0.0003; k2 = -0.0002	0.9915	0.0276

drying conditions (temperature, relative humidity, etc.) and the characteristics of the wet product (morphology, dimensional size, and moisture content). The linearization method applied to equation (12) was chosen to determine the effective moisture diffusivity coefficient (D_{eff}) values for different slice thicknesses. The linearized equation is expressed on the x-axis as ln(MR) and on the y-axis as time, as illustrated in Figure 7. The appropriate linear fitting resulted in coefficients of determination (R^2) of 0.9846, 0.9831, and 0.9613 for the direct solar dryer, and 0.9686, 0.9689, and 0.9540 for open sun drying at thicknesses of 5, 7, and 10 mm, respectively.

The slopes obtained from the plots were used to determine the effective moisture diffusivity (D_{eff}) using Equation (12), resulting in values of 1.65×10^{-8}, 2.66×10^{-8}, and 4.11×10^{-8} m^2/s for the direct solar dryer, and 0.89×10^{-8}, 1.52×10^{-8}, and 2.38×10^{-8} m^2/s for open sun drying at thicknesses of 5, 7, and 10 mm, respectively, as shown in Figure 8. The relationship between turmeric slice thickness and the effective moisture diffusivity coefficient indicates that thicker slices exhibited a

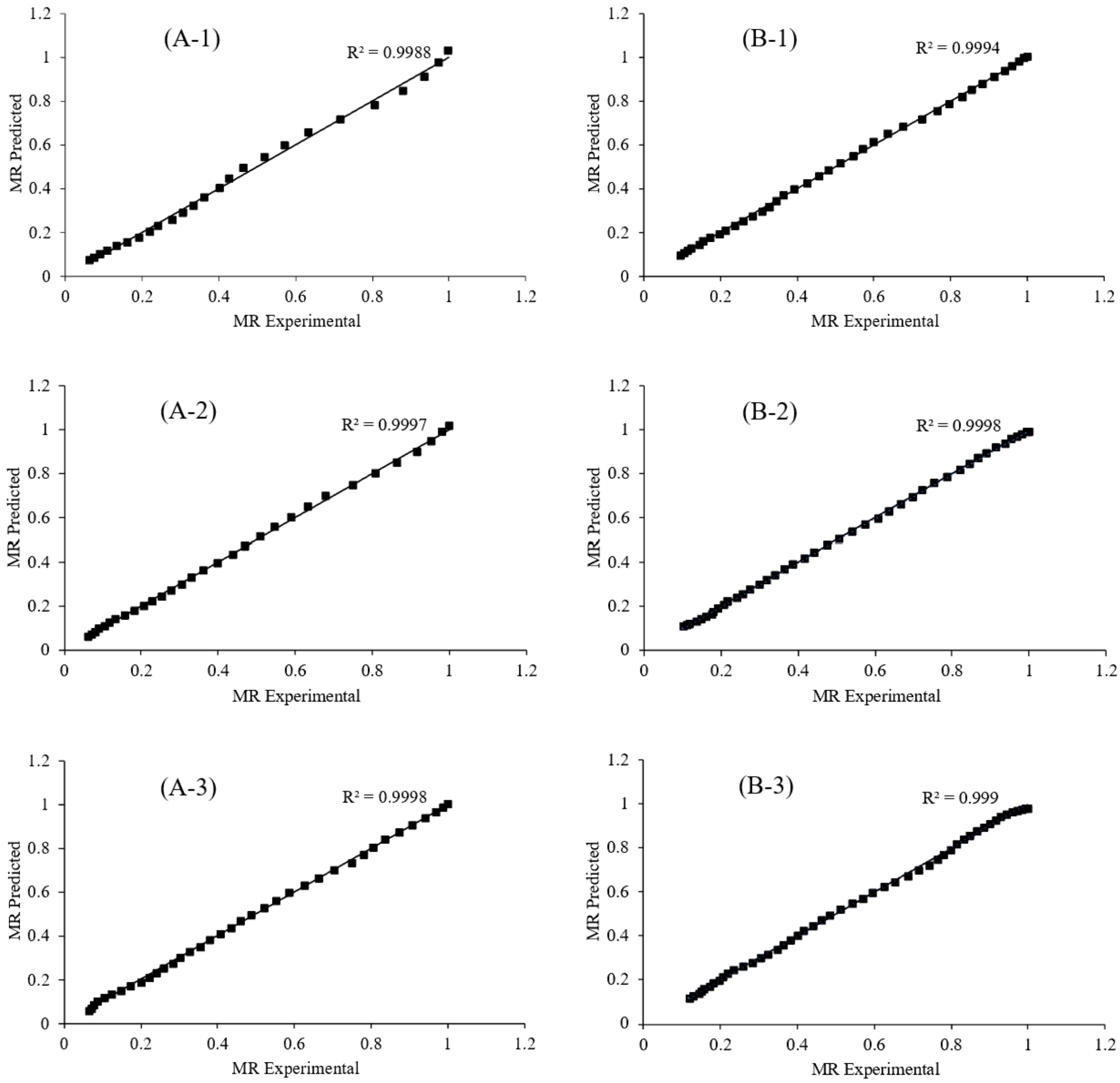

Fig. 6 Comparison of experimental MR and predicted MR from the Midilli model for drying turmeric slices using (A) photovoltaic-ventilated direct solar dryer and (B) open sun drying at thicknesses of 5 mm (1), 7 mm (2), and 10 mm (3)

Table 6
ANOVA results for the moisture diffusivity effective

Source of variation	SS	df	MS	F	P-value	F-crit
Between groups	2.96×10^{-15}	5	5.91×10^{-16}	1378.90	4.03×10^{-16}	3.11
Within groups	5.14×10^{-18}	12	4.29×10^{-19}			
Total	2.96×10^{-15}	17				

significantly higher diffusivity coefficient ($P < 0.05$), as shown in Table 6. Thicker turmeric slices exhibit increasing values of the diffusivity coefficient. Thicker slices can maintain a higher moisture gradient over a longer drying time. This gradient promotes the rate of moisture diffusion, thereby accelerating the drying process under the influence of the moisture content difference (Shen *et al.,* 2024). The D_{eff} values found in this study are consistent with previous studies conducted by (Abderrahman *et al.,* 2022), (Liu *et al.*, 2023), and (Sun *et al.,* 2025), and fall within the reported range of 10^{-11} to 10^{-6} m^2/s for various food products (Korese & Achaglinkame, 2024; Patel *et al.*, 2023).

3.6 Heat and mass transfer

The convective heat transfer coefficient (h_c) and evaporative heat transfer coefficient (h_e) for drying turmeric slices using a photovoltaic-ventilated direct solar dryer and open sun drying

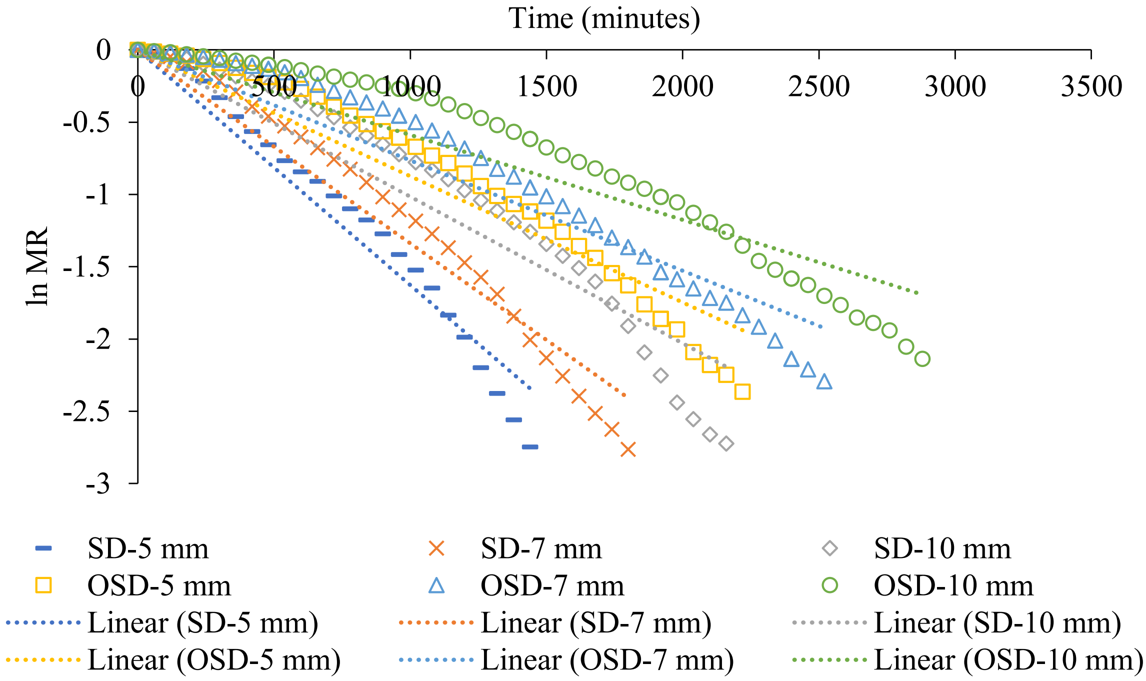

	SD-5 mm	SD-7 mm	SD-10 mm	OSD-5 mm	OSD-7 mm	OSD-10 mm
Equation	$y = -0.0016x$	$y = -0.0013x$	$y = -0.0010x$	$y = -0.0009x$	$y = -0.0008x$	$y = -0.0006x$
R^2	0.9846	0.9831	0.9613	0.9686	0.9689	0.954

Fig. 7 Plot of ln(MR) versus drying time for different drying methods at various material thicknesses

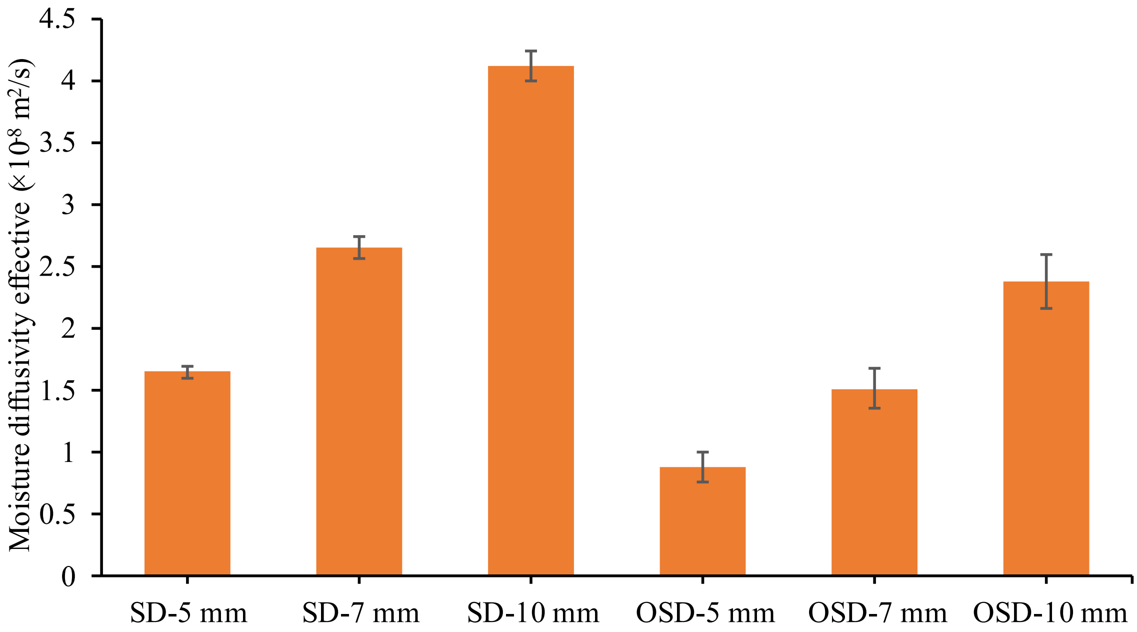

Fig. 8 Effect of material thickness and drying methods on effective moisture diffusivity

are presented in Figure 9 (A) and (B). The average h_c values for the direct solar dryer were 0.0498, 0.0481, and 0.0354 W/m².°C, while for open sun drying, they were 0.0475, 0.0381, and 0.0280 W/m².°C, respectively, at slice thicknesses of 5, 7, and 10 mm. Furthermore, the average h_e values obtained for the direct solar dryer were 20.785, 14.438, and 9.652 W/m².°C, while for open sun drying, they were 11.768, 9.919, and 8.191 W/m².°C, respectively, at the same slice thicknesses. The ANOVA test results in the effect of slice thickness and drying method on the values of h_c and h_e showed significant differences ($P < 0.05$), as shown in Table 7. The results indicate that both h_c and h_e

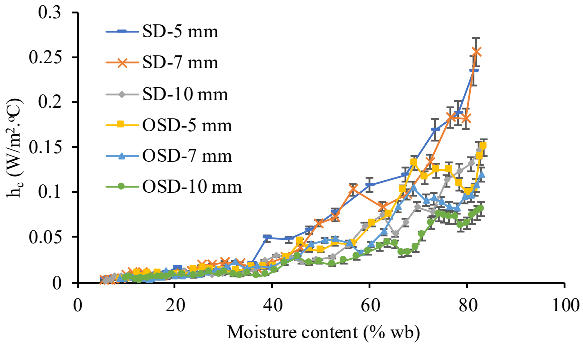

(A)

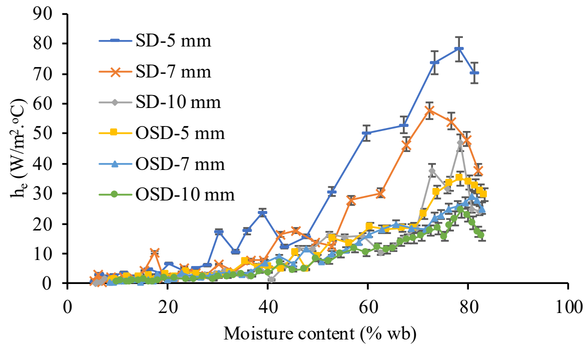

(B)

Fig. 9 Relationship between the moisture content of turmeric slices and the convective heat transfer coefficient (h_c) (A) and the evaporative heat transfer coefficient (h_e) (B)

Table 7
ANOVA results for the heat, evaporative and mass transfer coefficient

Source of variation	SS	df	MS	F	P-value	F-crit
1. Heat transfer coefficient (h_c)						
Between groups	1.16×10^{-3}	5	2.32×10^{-4}	4.85	0.012	3.11
Within groups	5.74×10^{-4}	12	4.78×10^{-5}			
Total	1.73×10^{-3}	17				
2. Evaporative heat transfer coefficient (h_e)						
Between groups	319.06	5	63.81	143.27	2.87×10^{-10}	3.11
Within groups	5.34	12	0.44			
Total	324.40	17				
3. Mass transfer coefficient (h_m)						
Between groups	3.13×10^{-12}	5	6.26×10^{-13}	3.52	0.034	3.11
Within groups	2.13×10^{-12}	12	1.78×10^{-13}			
Total	5.26×10^{-12}	17				

decrease as the moisture content of the turmeric slices decreases, with thinner slices showing higher values of h_c and h_e. One operational condition that affects the values of h_c and h_e during the drying process is the amount of moisture mass removed; at the beginning of the drying period, the moisture content is still high, leading to a higher amount of moisture being evaporated, which increases the value of h_c. As time progresses, the moisture content decreases. The drying process occurs under natural convection conditions, where the drying air convection flow is identified using the Grashof number (Gr) and Prandtl number (Pr). The Grashof number ranges from 1081.93 to 19785.90, while the Prandtl number remains stable

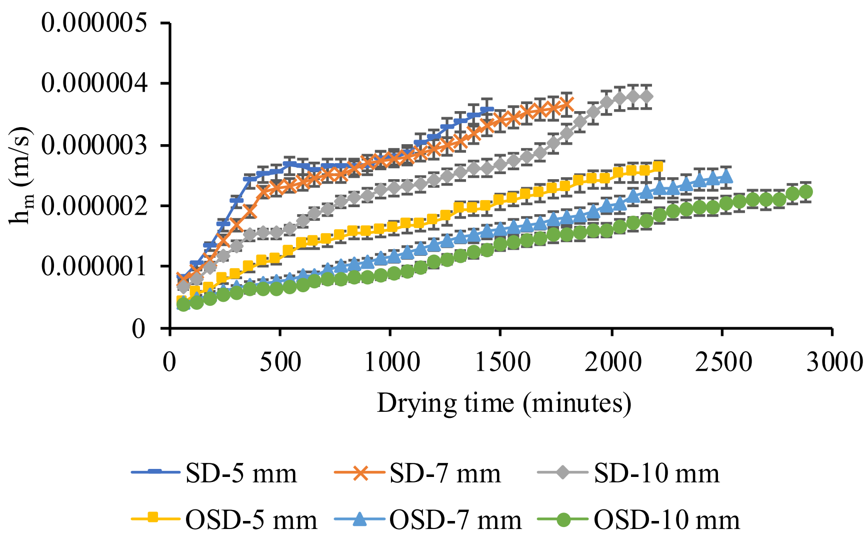

Fig. 10 Mass transfer coefficient (h_m) values during the drying process

in the range of 0.705 to 0.706 during the drying process. The product of the Gr and Pr numbers falls within the range of GrPr ≤ 10^7, indicating a laminar flow regime during drying (Jain, 2006; Malik & Kumar, 2024a).

Figure 10 shows the variation of the mass transfer coefficient (h_m) over time during the drying of turmeric slices with different slice thicknesses and drying methods. The average h_m values for the direct solar dryer were 2.54 × 10^{-6}, 2.59 × 10^{-6}, and 2.34 × 10^{-6} m/s for thicknesses of 5, 7, and 10 mm, respectively, while the open sun drying yielded values of 1.70 × 10^{-6}, 1.43 × 10^{-6}, and 1.29 × 10^{-6} m/s for the same thicknesses. ANOVA test results showed that slice thickness and drying method significantly affected the hm values ($P < 0.05$), as shown in Table 7. The value of h_m increases as the drying time progresses, with higher values observed for thinner slices. Thinner turmeric slices have a larger surface area, allowing faster mass transfer within the sample (Sun *et al.*, 2025). During the initial drying period, there is an adjustment or initial heating phase, and the drying air temperature increases in the subsequent period, causing the temperature of the moist food material to rise as drying time increases. The rise in temperature of the moist food generates a temperature gradient between the food and the drying air, which can improve moisture diffusivity and accelerate the moisture removal rate from the material's surface (Koua *et al.*, 2019).

4. Conclusion

This study evaluates the drying characteristics and mathematical modeling to describe the behavior, performance, and phenomena during the drying process. A photovoltaic ventilation direct solar dryer was developed and constructed for drying turmeric slices, and it was compared with the open sun drying method. The initial moisture content of the turmeric slices was 83.48%, which was dehydrated to achieve a final moisture content of 5-6% to ensure safe storage conditions. Turmeric was sliced into different thicknesses—5, 7, and 10 mm—requiring drying times to reach their respective final moisture content limits of 1440 min, 1800 min, and 2160 min for the direct solar dryer, and 2220 min, 2520 min, and 2880 min for open sun drying. Turmeric slices dried using the direct solar dryer showed a faster drying rate compared to the open sun drying method, with the highest average drying rate observed for the 5 mm slices at 0.287 g/min, followed by 0.229 g/min for the 7 mm slices and 0.191 g/min for the 10 mm slices. The performance of the solar dryer was expressed in terms of drying efficiency, which showed a higher value for the 5 mm thickness; however, the result was still considered low, indicating the need for optimisation of the drying chamber on a larger scale to maximise solar energy utilisation. Thin-layer drying modeling revealed that the Midilli model provided the most accurate representation based on statistical analysis for drying turmeric slices using the direct solar dryer with photovoltaic ventilation and open sun drying at various slice thicknesses. The effective moisture diffusivity obtained in this study was 1.65 × 10^{-8}, 2.66 × 10^{-8}, and 4.11 × 10^{-8} m^2/s for the direct solar dryer, and 0.89 × 10^{-8}, 1.52 × 10^{-8}, and 2.38 × 10^{-8} m^2/s for open sun drying, at thicknesses of 5, 7, and 10 mm respectively, indicating that these diffusivity values fall within the appropriate range for food product drying. The convective heat transfer coefficient (h_c) and the evaporative heat transfer coefficient (h_e) decreased as the moisture content of the turmeric slices decreased for all drying methods and thickness variations. Meanwhile, the mass transfer coefficient (h_m) increased with drying time. Higher heat and mass transfer coefficient values were observed for drying thinner turmeric slices, both with the direct solar dryer and open sun drying.

Acknowledgments

The authors are very grateful to the Department of Chemical Engineering, Diponegoro University, for providing facilities for this research. The authors also thank the advisor who provided input to complete this scientific article. The authors are also very grateful to Diponegoro University for funding the International Scientific Publication (RPI) project scheme with a contract number 1145/UN7.D2/PP/XI/2024.

Author Contributions: B.W.H.E.P.; supervision, funding acquisition, investigation, validation, writing – review & editing, S.S.; supervision, conceptualization, project administration, writing—review and editing, B.J.; supervision, investigation, validation, writing—review and editing, M.A.A.; methodology, data curation, visualization, writing—original draft. All authors have read and agreed to the published version of the manuscript.

Funding: This research was supported by Diponegoro University for funding the International Scientific Publication (RPI) project scheme. [Grant number: 1145/UN7.D2/PP/XI/2024]

Conflicts of Interest: The authors declare no conflict of interest.

References

Abderrahman, M., Abdelaziz, B., & Abdelkader, O. (2022). Thermal performances and kinetics analyses of greenhouse hybrid drying of two-phase olive pomace: Effect of thin layer thickness. *Renewable Energy*, *199*, 407–418. https://doi.org/10.1016/j.renene.2022.09.012

Admass, Z., Salau, A. O., Mhari, B., & Tefera, E. (2024). Red pepper drying with a double pass solar air heater integrated with aluminium cans. *Scientific Reports*, *14*(1), 2877. https://doi.org/10.1038/s41598-024-53563-6

Ambawat, S., Sharma, A., & Saini, R. K. (2022). Mathematical Modeling of Thin Layer Drying Kinetics and Moisture Diffusivity Study of Pretreated Moringa oleifera Leaves Using Fluidized Bed Dryer. *Processes*, *10*(11), 2464. https://doi.org/10.3390/pr10112464

Arunkumar, P. M., Balaji, N., & Madhankumar, S. (2024). Performance analysis of indirect solar dryer with natural heat energy retention substances for drying red chilli. *Sustainable Energy Technologies and Assessments*, *64*, 103706. https://doi.org/10.1016/j.seta.2024.103706

Bhaskara Rao, T. S. S., & Murugan, S. (2021). Solar drying of medicinal herbs: A review. In *Solar Energy* (Vol. 223, pp. 415–436). Elsevier Ltd. https://doi.org/10.1016/j.solener.2021.05.065

Borah, A., Hazarika, K., & Khayer, S. M. (2015). Drying kinetics of whole and sliced turmeric rhizomes (Curcuma longa L.) in a solar conduction dryer. *Information Processing in Agriculture*, *2*(2), 85–92. https://doi.org/10.1016/j.inpa.2015.06.002

BPS. (2024). *Produksi Tanaman Biofarmaka Menurut Jenis Tanaman, 2023*.

Chicco, D., Warrens, M. J., & Jurman, G. (2021). The coefficient of determination R-squared is more informative than SMAPE, MAE, MAPE, MSE and RMSE in regression analysis evaluation. *PeerJ Computer Science*, *7*, e623. https://doi.org/10.7717/peerj-cs.623

Choudhary, A. K., & Hazarika, M. K. (2024). Modelling and thermal analysis of an integrated solar greenhouse dryer for ginger (Zingiber officinale) and product quality. *Journal of Stored Products Research*, *106*, 102313. https://doi.org/10.1016/j.jspr.2024.102313

Daş, M., Alıç, E., & Kavak Akpinar, E. (2021). Numerical and experimental analysis of heat and mass transfer in the drying process of the solar drying system. *Engineering Science and*

Technology, an International Journal, *24*(1), 236–246. https://doi.org/10.1016/j.jestch.2020.10.003

Deepak, C. N., & Behura, A. K. (2025). Effect on drying kinetics and product quality of cucumber in a mixed mode solar tunnel dryer upon integration of sensible and latent heat thermal energy storage. *Solar Energy*, *285*, 113113. https://doi.org/10.1016/j.solener.2024.113113

Dutta, C., Yadav, D. K., Arora, V. K., & Malakar, S. (2023). Drying characteristics and quality analysis of pre-treated turmeric (Curcuma longa) using evacuated tube solar dryer with and without thermal energy storage. *Solar Energy*, *251*, 392–403. https://doi.org/10.1016/j.solener.2023.01.032

Ebadi, H., Zare, D., Ahmadi, M., & Chen, G. (2021). Performance of a hybrid compound parabolic concentrator solar dryer for tomato slices drying. *Solar Energy*, *215*, 44–63. https://doi.org/10.1016/j.solener.2020.12.026

Efendi, M. (2024). Influence of glazing type on the drying kinetics and thermal performance of indirect solar dryer for jelly candy. *Renewable Energy*, *231*, 120950. https://doi.org/10.1016/j.renene.2024.120950

Gasa, S., Sibanda, S., Workneh, T. S., Laing, M., & Kassim, A. (2022). Thin-layer modelling of sweet potato slices drying under naturally-ventilated warm air by solar-venturi dryer. *Heliyon*, *8*(2). https://doi.org/10.1016/j.heliyon.2022.e08949

Hasan Masud, M., Karim, A., Ananno, A. A., & Ahmed, A. (2020). *Sustainable Food Drying Techniques in Developing Countries: Prospects and Challenges*. Springer International Publishing. https://doi.org/10.1007/978-3-030-42476-3

Hasibuan, R., Haryanto, B., Nafsun, A. I. binti, Pramananda, V., Siregar, F. F., & Fazillah, R. (2025). Drying of red ginger slices using tray dryer integrated with pyrolysis reactor as a heat source: Evaluation on the drying characteristics, red ginger quality, and drying kinetics. *Case Studies in Chemical and Environmental Engineering*, *11*, 101055. https://doi.org/10.1016/j.cscee.2024.101055

Hssaini, L., Ouaabou, R., Hanine, H., Razouk, R., & Idlimam, A. (2021). Kinetics, energy efficiency and mathematical modeling of thin layer solar drying of figs (Ficus carica L.). *Scientific Reports*, *11*(1), 21266. https://doi.org/10.1038/s41598-021-00690-z

Jain, D. (2006). Determination of Convective Heat and Mass Transfer Coefficients for Solar Drying of Fish. *Biosystems Engineering*, *94*(3), 429–435. https://doi.org/10.1016/j.biosystemseng.2006.04.006

Jeevarathinam, G., Pandiselvam, R., Pandiarajan, T., Preetha, P., Balakrishnan, M., Thirupathi, V., & Kothakota, A. (2021). Infrared assisted hot air dryer for turmeric slices:Effect on drying rate and quality parameters. *LWT*, *144*, 111258. https://doi.org/10.1016/j.lwt.2021.111258

Jha, A., & Tripathy, P. P. (2021). Recent Advancements in Design, Application, and Simulation Studies of Hybrid Solar Drying Technology. *Food Engineering Reviews*, *13*(2), 375–410. https://doi.org/10.1007/s12393-020-09223-2

Kern, D. Q. (1965). *Process Heat Transfer*. McGraw-Hill Book Company, Inc.

Kerse, A. Y., Embiale, D. T., & Gunjo, D. G. (2025). Dehydration of red chilli using an indirect type forced convection solar dryer integrated with thermal energy storage. *International Journal of Thermofluids*, *26*, 101045. https://doi.org/10.1016/j.ijft.2024.101045

Khater, E.-S. G., Bahnasawy, A. H., Oraiath, A. A. T., Alhag, S. K., Al-Shuraym, L. A., Moustapha, M. E., Elwakeel, A. E., Elbeltagi, A., Salem, A., Metwally, K. A., Abdalla, M. A. I., Hussein, M. M., & Abdeen, M. A. (2024). Assessment of a LPG hybrid solar dryer assisted with smart air circulation system for drying basil leaves. *Scientific Reports*, *14*(1), 23922. https://doi.org/10.1038/s41598-024-74751-4

Komonsing, N., Khuwijitjaru, P., Nagle, M., Müller, J., & Mahayothee, B. (2022). Effect of drying temperature together with light on drying characteristics and bioactive compounds in turmeric slice. *Journal of Food Engineering*, *317*. https://doi.org/10.1016/j.jfoodeng.2021.110695

Korese, J. K., & Achaglinkame, M. A. (2024). Convective drying of Gardenia erubescens fruits: Effect of pretreatment, slice thickness and drying air temperature on drying kinetics and product quality. *Heliyon*, *10*(4), e25968. https://doi.org/10.1016/j.heliyon.2024.e25968

Koua, B. K., Koffi, P. M. E., & Gbaha, P. (2019). Evolution of shrinkage, real density, porosity, heat and mass transfer coefficients during indirect solar drying of cocoa beans. *Journal of the Saudi Society of Agricultural Sciences*, *18*(1), 72–82. https://doi.org/10.1016/j.jssas.2017.01.002

Koukouch, A., Idlimam, A., Asbik, M., Sarh, B., Izrar, B., Bostyn, S., Bah, A., Ansari, O., Zegaoui, O., & Amine, A. (2017). Experimental determination of the effective moisture diffusivity and activation energy during convective solar drying of olive pomace waste. *Renewable Energy*, *101*, 565–574. https://doi.org/10.1016/j.renene.2016.09.006

Lakshmi, D. V. N., Muthukumar, P., Layek, A., & Nayak, P. K. (2018). Drying kinetics and quality analysis of black turmeric (Curcuma caesia) drying in a mixed mode forced convection solar dryer integrated with thermal energy storage. *Renewable Energy*, *120*, 23–34. https://doi.org/10.1016/j.renene.2017.12.053

Lingayat, A., Balijepalli, R., & Chandramohan, V. P. (2021). Applications of solar energy based drying technologies in various industries – A review. In *Solar Energy* (Vol. 229, pp. 52–68). Elsevier Ltd. https://doi.org/10.1016/j.solener.2021.05.058

Lingayat, A., Zachariah, R., & Modi, A. (2022). Current status and prospect of integrating solar air heating systems for drying in various sectors and industries. *Sustainable Energy Technologies and Assessments*, *52*, 102274. https://doi.org/10.1016/j.seta.2022.102274

Liu, D., Wang, Q., Hu, A., Wang, Z., Zhang, Q., & Wang, L. (2023). Optimized model of sludge drying characteristics based on an experimental study of thickness, temperature, and humidity. *Journal of Cleaner Production*, *429*, 139540. https://doi.org/10.1016/j.jclepro.2023.139540

Madhankumar, S., Viswanathan, K., Wu, W., & Ikhsan Taipabu, M. (2023). Analysis of indirect solar dryer with PCM energy storage material: Energy, economic, drying and optimization. *Solar Energy*, *249*, 667–683. https://doi.org/10.1016/j.solener.2022.12.009

Malik, A., & Kumar, M. (2024a). Assessment of a mixed-mode vertical solar dryer for experimental turmeric drying. *Solar Energy*, *282*, 112980. https://doi.org/10.1016/j.solener.2024.112980

Malik, A., & Kumar, M. (2024b). Experimental ginger drying by a novel mixed-mode vertical solar dryer under partial and fully loaded conditions. *Innovative Food Science & Emerging Technologies*, *95*, 103736. https://doi.org/10.1016/j.ifset.2024.103736

Midilli, A., Kucuk, H., & Yapar, Z. (2002). A new model for single-layer drying. *Drying Technology*, *20*(7), 1503–1513. https://doi.org/10.1081/DRT-120005864

Öksüz, H. B., & Buzrul, S. (2024). DrYFiT : An Excel Freeware Tool to Describe Thin Layer Drying of Foods. *Journal of Food Process Engineering*, *47*(10). https://doi.org/10.1111/jfpe.14748

Patel, V., Judal, K. B., Panchal, H., Singh, B., Jomde, A., Kumar, A., Patel, A., Jain, R., & Sadasivuni, K. K. (2023). Investigation on drying kinetics analysis of gooseberry slices dried under open sun. *Environmental Challenges*, *13*, 100778. https://doi.org/10.1016/j.envc.2023.100778

Perussello, C. A., Kumar, C., de Castilhos, F., & Karim, M. A. (2014). Heat and mass transfer modeling of the osmo-convective drying of yacon roots (Smallanthus sonchifolius). *Applied Thermal Engineering*, *63*(1), 23–32. https://doi.org/10.1016/j.applthermaleng.2013.10.020

Perussello, C. A., Mariani, V. C., & do Amarante, Á. C. C. (2012). Numerical and experimental analysis of the heat and mass transfer during okara drying. *Applied Thermal Engineering*, *48*, 325–331. https://doi.org/10.1016/j.applthermaleng.2012.04.025

Poonia, S., Singh, A. K., & Jain, D. (2018). Design development and performance evaluation of photovoltaic/thermal (PV/T) hybrid solar dryer for drying of ber (*Zizyphus mauritiana)* fruit. *Cogent Engineering*, *5*(1), 1507084. https://doi.org/10.1080/23311916.2018.1507084

Sharma, S., Dhalsamant, K., Tripathy, P. P., & Manepally, R. K. (2021). Quality analysis and drying characteristics of turmeric (Curcuma longa L.) dried by hot air and direct solar dryers. *LWT*, *138*. https://doi.org/10.1016/j.lwt.2020.110687

Shen, C., Chen, W., Aziz, T., Khojah, E., Al-Asmari, F., Alamri, A. S., Alhomrani, M., Cui, H., & Lin, L. (2024). Drying kinetics and moisture migration mechanism of yam slices by cold plasma pretreatment combined with far-infrared drying. *Innovative Food Science & Emerging Technologies*, *95*, 103730. https://doi.org/10.1016/j.ifset.2024.103730

Shimpy, Kumar, M., & Kumar, A. (2024). Assessment of a beeswax-packed domestic solar dryer for sustainable bitter gourd drying: An experimental study. *Food and Bioproducts Processing*, *148*, 72–87. https://doi.org/10.1016/j.fbp.2024.08.007

Singh, P., & Gaur, M. K. (2021). Environmental and economic analysis of novel hybrid active greenhouse solar dryer with evacuated tube solar collector. *Sustainable Energy Technologies and Assessments*, *47*. https://doi.org/10.1016/j.seta.2021.101428

Suherman, S., Asy-Syaqiq, M. A., Rahayu, E., Simanjuntak, Z., Sussardi, A. R., Hadiyanto, H., Prasetiyono, B. W. H. E., & Saptoro, A. (2024). Performance of a mixed-mode air recirculation solar dryer integrated with thermal energy storage and evacuated tube solar collector for drying sweet corn kernels. *Journal of Food Science and Technology*. https://doi.org/10.1007/s13197-024-06090-1

Suherman, S., Susanto, E. E., Ayu, A. D., & Dea, S. (2021). Experimental investigation of ginger drying using hybrid solar dryer. *Journal of Applied Science and Engineering (Taiwan)*, *24*(4), 553–564. https://doi.org/10.6180/jase.202108_24(4).0011

Suherman, S., Susanto, E. E., Zardani, A. W., Dewi, N. H. R., & Hadiyanto, H. (2020). Energy–exergy analysis and mathematical modeling of cassava starch drying using a hybrid solar dryer. *Cogent Engineering*, *7*(1). https://doi.org/10.1080/23311916.2020.1771819

Sun, J., Wang, Y., Wang, Y., Liu, C., Ma, S., & Ma, H. (2025). Effects of temperature, relative humidity, and sludge thickness on sludge drying characteristics and kinetic investigation. *Chemical Engineering Research and Design*, *214*, 177–187. https://doi.org/10.1016/j.cherd.2024.12.038

Tagnamas, Z., Idlimam, A., & Lamharrar, A. (2024). Effect of microwave pretreatment on truffle solar drying from an energetic perspective. *Food Frontiers*, *5*(3), 994–1003. https://doi.org/10.1002/fft2.390

Turmeric outlook. (2024). *Turmeric Seasonal Report: 2024*.

Vigneshkumar, N., Venkatasudhahar, M., Manoj Kumar, P., Ramesh, A., Subbiah, R., Michael Joseph Stalin, P., Suresh, V., Naresh Kumar, M., Monith, S., Manoj kumar, R., & Kriuthikeswaran, M. (2021). Investigation on indirect solar dryer for drying sliced potatoes using phase change materials (PCM). *Materials Today: Proceedings*, *47*, 5233–5238. https://doi.org/10.1016/j.matpr.2021.05.562

LIST OF APPENDICES

Appendix A

The following expressions are used to calculate the values of statistical parameters.

$$R^2 = 1 - \left(\frac{\sum_{i=1}^{N}(MR_{exp,i}-MR_{pre,i})^2}{\sum_{i=1}^{N}(\overline{MR_{1,exp}}-MR_{exp,i})^2}\right) \quad (A.1)$$

$$RMSE = \left(\frac{\sum_{i=1}^{N}(MR_{pre,i}-MR_{exp,i})^2}{N}\right)^{\frac{1}{2}} \quad (A.2)$$

N = Number of observations in an experiment.

Appendix B

The Grashof number (Gr), Prandtl number (Pr), and the thermophysical properties of moist air, such as density (ρ_v, kg/m^3), thermal conductivity (K_v, W/m.°C), specific heat ($\mathbf{C_v}$, J/kg.°C), dynamic viscosity (μ_v, kg/m.s), the partial vapour pressure at T temperature (P(T), N/m^2), latent heat (λ, J/kg), are determined by the polynomial equations from equations (B.1) to (B.8).

$$Pr = \frac{\mu_v C_v}{K_v} \quad (B.1)$$

$$Gr = \frac{L^3 g\beta(T-T_a)}{\mu^2} \quad (B.2)$$

$$\rho_v = \frac{353.44}{(T_i+273.15)} \quad (B.3)$$

$$K_v = 0.0244 + 0.6773 \times 10^{-4} T_i \quad (B.4)$$

$$C_v = 999.2 + 0.1434T_i + 1.101 \times 10^{-4} T_i^2 - 6.7581 \times 10^{-8} T_i^3 \quad (B.5)$$

$$\mu_v = 1.718 \times 10^{-5} + 4.620 \times 10^{-8} T_i \quad (B.6)$$

$$P(T) = \exp\left(25.317 - \frac{5144}{T+273.15}\right) \quad (B.7)$$

$$\lambda = (2500.82 - 2.358 \times T_i)10^3 \quad (B.8)$$

The temperature T_i is the value obtained from the average surface temperature of the product (T_{ps}) and the temperature above the product surface (T_{aps}).

Appendix C

The ANOVA parameters were calculated using the following equations.

$$\text{Total (T)} = X_1 + X_2 + X_3 \quad (C.1)$$

$$\text{Correction factor} = \left(\frac{T^2}{M}\right) \quad (C.2)$$

$$\text{Sum of square between samples (SSC)} = \frac{(\Sigma X_1)^2}{n_1} + \frac{(\Sigma X_2)^2}{n_2} + \frac{(\Sigma X_3)^2}{n_3} - \frac{T^2}{M} \quad (C.3)$$

$$\text{Degree of freedom (df) for SSC} = E - 1 \quad (C.4)$$

$$\text{Total sum of square (SST)} = \Sigma X_1^2 + \Sigma X_2^2 + \Sigma X_3^2 - \frac{T^2}{M} \quad (C.5)$$

$$\text{Degree of freedom (df) for SST} = M - 1 \quad (C.6)$$

$$\text{Sum of square with in samples (SSE)} = SST - SSC \quad (C.7)$$

$$\text{Degree of freedom (df) for SSE} = M - E \quad (C.8)$$

$$\text{Mean sum of square between samples (MSC)} = \frac{SSC}{E-1} \quad (C.9)$$

$$\text{Mean sum of square with in sampels} = \frac{SSE}{M-E} \quad (C.10)$$

$$p - \text{value} = \frac{MSC}{MSE} \quad (C.11)$$

where X_1, X_2, and X_3 are the data value, M is the total number of samples, n_1, n_2, and n_3 are the number of samples per run, and E is the number of experimental runs.